The Astrophysical Journal, 678: L97–L100, 2008 May 10

THE MID-INFRARED FUNDAMENTAL PLANE OF EARLY-TYPE GALAXIES

Hyunsung David Jun[1] and Myungshin Im[1,2]

Received 2007 December 9; accepted 2008 March 25; published 2008 April 10

ABSTRACT

Three observables of early-type galaxies—size (r_e), surface brightness (I_e), and velocity dispersion (σ_0)—form a tight planar correlation known as the fundamental plane (FP), which has provided great insights into the galaxy formation and the evolution processes. However, the FP has been found to be tilted against the simple virial expectation, prompting debates on its origin. In order to investigate the contribution of systematic stellar population variation to the FP tilt, we study here the FP relations of early-type galaxies in the mid-infrared (MIR), which may represent stellar mass well. We examine the wavelength dependence of the FP coefficients a and b in $\log r_e = a \log \sigma_0 + b \log \langle I \rangle_e + c$, using a sample of 56 early-type galaxies for which visible (V band), near-infrared (K band), and MIR (*Spitzer* IRAC, 3.6–8.0 μm) data are available. We find that the coefficient a increases as a function of wavelength as $da/d\lambda = 0.11 \pm 0.04\ \mu\mathrm{m}^{-1}$, while the coefficient b reaches the closest to -1 at 3.6–5.8 μm. When applied to the visible FP coefficients derived from a larger sample of nearby early-type galaxies, we get the FP relation with $(a, b) \simeq (1.6\text{–}1.8, -0.9)$ at 3.6 μm. Our result suggests that the stellar population effect can explain more than half of the FP tilt, closing the gap between the virial expectation and the optical FP. The reduction in the FP tilt is reflected in the dynamical mass-to-light ratio, M_{dyn}/L, dependence on L which decreases toward 3.6–5.8 μm, suggesting that the MIR light better represents mass than the shorter wavelengths.

Subject headings: galaxies: elliptical and lenticular, cD — galaxies: formation — galaxies: fundamental parameters — galaxies: stellar content — galaxies: structure — infrared: galaxies

Online material: color figure

1. INTRODUCTION

In the search for correlations among physical parameters of early-type galaxies, it has been recognized that the effective radius (r_e), the effective mean surface brightness ($\langle I \rangle_e$), and the central velocity dispersion (σ_0) form a planar relation (in logarithmic space) known as the fundamental plane (hereafter FP; Dressler et al. 1987; Djorgovski & Davis 1987), in the form of $r_e \propto \sigma_0^a \langle I \rangle_e^b$ where a and b are found to be $(a, b) \simeq (1.2\text{–}1.5, -0.8)$ at visible wavelengths (Jørgensen et al. 1996; Bernardi et al. 2003). Under the assumption of structural homology and a constant mass-to-light ratio, the virial theorem implies that the FP coefficients should be $(a, b) = (2, -1)$—the so-called virial expectation. The observed discrepancy, or tilt of the FP with respect to the virial expectation, has prompted many discussions to explain its origin (see D'Onofrio et al. [2006] for a review of this field).

One of the ideas is that the tilt is caused by the systematic variation in the stellar population as a function of physical parameters such as galaxy luminosity. Pahre et al. (1998a) investigated this effect by constructing the FP in K band, which is supposedly a good tracer of the stellar mass less affected by age and dust. Meanwhile, Scodeggio et al. (1998) examined the wavelength dependence of the FP coefficients, and concluded that some of the tilt is caused by the stellar population manifested by the color-magnitude relation. These studies found that the stellar population effect exists, but it can only partially explain the tilt of the FP.

More recent investigations tackle the FP tilt problem using new methods such as gravitational lensing (Treu et al. 2006; Bolton et al. 2007) or dynamical modeling (Padmanabhan et al. 2004; Cappellari et al. 2006). Such studies suggest that the FP tilt nearly disappears when the FP is constructed in the mass domain. Their conclusion is that the tilt must arise from the variation in the central mass-to-light ratio (Robertson et al. 2006), but it is not clear whether the variation is dominated by dark matter or by stars (Bolton et al. 2007).

In this Letter, we extend the FP analysis to wavelengths beyond K band to further investigate the effect of stellar population on the tilt. By doing so we aim to provide the FP that possibly better represents stellar mass (see § 5), and to improve the constraints on different scenarios for the FP tilt.

2. THE SAMPLE

Early-type galaxies were chosen from the sample of Pahre (1999), which was used to study the FP of nearby early-type galaxies in visible and near-infrared (hereafter NIR) passbands. The sample has the velocity dispersion information necessary for constructing the FP. We then searched for mid-infrared (hereafter MIR)[3] archival images for galaxies in the Pahre (1999) sample. For the MIR data, we used the *Spitzer Space Telescope* Infrared Array Camera (hereafter IRAC; Fazio et al. 2004) images, covering four wavelength channels at 3.6, 4.5, 5.8, and 8.0 μm. The flux-calibrated, mosaicked IRAC images were retrieved from the *Spitzer* archive for these objects.

The surface brightness fitting was performed for these matched galaxies, and the objects satisfying $r_e > 2''$ for three or more IRAC bands were retained for the FP analysis. We imposed this size limit in order to work with a sample with reliable r_e values (see § 3.1). After removing a few galaxies (NGC

[1] Astronomy Program, Department of Physics and Astronomy, FPRD, Seoul National University, Seoul 151-742, Korea; hsjun@astro.snu.ac.kr, mim@astro.snu.ac.kr.

[2] Infrared Processing and Analysis Center, California Institute of Technology, Pasadena, CA 91125.

[3] We designate these wavelengths MIR to distinguish them from the K band.

1275, NGC 4824, NGC 4478, and NGC 6166) that show peculiar light profiles (multiple source, close to a bright galaxy or stars), we finally identified 56 galaxies with IRAC data in five clusters (A0426, A1656, A2199, A2634, and Virgo) satisfying our selection criteria. We present a brief summary of the photometric information in Table 1. The exposure times for the IRAC data range from 72 to 1000 s.

The above selection of the sample may introduce a bias in the derived FP coefficients (Scodeggio et al. 1998). However, such a bias would not affect our derivation of the wavelength dependence of the FP coefficients, since the multiwavelength FP coefficients will be derived from the same galaxies for which the same bias would apply.

3. ANALYSIS OF THE DATA

3.1. *Surface Brightness Fitting*

IRAF ELLIPSE was used to obtain surface brightness profiles of our IRAC sample galaxies. We restricted the fitting region to $a > 2$ pixels (along the semimajor axis) and discarded regions with $S/N_{rms} < 1$. During the fit, we held the center and fixed the ellipticities and the position angles of isophotes to those at the effective radius in the 3.6 μm band. In addition, 3 σ clipping was applied to reject outliers such as foreground stars. To subtract the background, we used the values determined from SExtractor (Bertin & Arnouts 1996). The adaptive background mesh sizes were varied between 16 and 96 pixels, and the best mesh was chosen to be the one which flattened the growth curve at the largest isophote [$a \sim (3\text{–}6)a_e$].

After the ELLIPSE photometry, we used the de Vaucouleurs $r^{1/4}$ law to fit the observed surface brightness profiles measured along the semimajor axis.[4] The fitting procedure yields the effective radius (in arcseconds) $r_e = \sqrt{(b/a)_e}\, a_e$ where a_e is the effective semimajor axis and $(b/a)_e$ is the axis ratio of the isophote at this position. We tested the reliability of our fitting procedure using the simulated, PSF-convolved galaxies, and found that the surface brightness fitting gives unbiased, reliable results when $r_e > 2''$. At the same time, we get the mean surface brightness within r_e (in AB magnitudes) $\langle\mu\rangle_e = m_{1/2} + 2.5 \log(\pi r_e^2) - 10 \log(1+z) - A_\lambda - K(z)$ where $m_{1/2}$ is the magnitude of the total flux within the effective isophote defined by a_e and b_e, while cosmological dimming, Galactic extinction (A_λ, using the formula of Laureijs et al. [1994] and the extinction curve of Fitzpatrick & Massa [2007]), and K-correction are taken into account. The K-correction is computed using the spectral energy distribution of a 13 Gyr age, solar metallicity, and 0.1 Gyr burst model from Bruzual & Charlot (2003) assuming the Salpeter initial mass function. The last observable, σ_0, is a kinematic parameter and is not expected to vary as a function of wavelength; we consequently use the same data used for the visible and NIR bands (Pahre 1999).

In our analysis, angular sizes were converted into physical length units for the FP construction by setting the distance to A1656 as 98.1 Mpc and calibrating the distances to individual clusters, utilizing the NIR FP (Pahre et al. 1998b) as a distance ladder.

[4] We also tried the Sérsic $r^{1/n}$ law but found no difference in the FP coefficients; we therefore kept the $r^{1/4}$ methodology.

TABLE 1
PHOTOMETRIC PARAMETERS OF THE SAMPLE

λ (μm)	$r_{e,\min}$ (arcsec)	$r_{e,\mathrm{avg}}$ (arcsec)	$r_{e,\max}$ (arcsec)	$M_{\min}$ (mag)	M_{avg} (mag)	$M_{\max}$ (mag)
0.55	2.1	20.1	81.1	−23.4	−21.4	−19.4
2.2	2.3	14.8	104.0	−26.7	−24.5	−22.6
3.6	2.0	14.3	65.3	−25.8	−23.6	−21.8
4.5	2.2	14.7	80.5	−25.1	−23.0	−21.2
5.8	1.2	15.2	90.0	−25.1	−22.7	−21.0
8.0	1.1	13.6	86.8	−24.2	−22.3	−20.5

NOTES.—Effective radii and absolute magnitudes from Pahre (1999) (V and K bands) and our *Spitzer* IRAC analysis (3.6–8.0 μm) are presented in minimum, average, and maximum values.

3.2. *Fitting of FP Coefficients*

We fitted the FP coefficients of the multi-wave-band sample in the following manner using a variety of methods:

$$\log r_e = a \log \sigma_0 + b \log \langle I\rangle_e + c, \tag{1}$$

where $\langle\mu\rangle_e$ and $\langle I\rangle_e$ are related as $\langle\mu\rangle_e \propto -2.5 \log \langle I\rangle_e$. For the input r_e and $\langle I\rangle_e$, we use our SB-fit results for MIR (§ 3.1), and those listed in Pahre (1999) for V and K bands. We tried five different fitting methods: standard least-squares fit, the inverse least-squares fit, the bisector of the two, the least-squares fit to the orthogonal plane, and the least absolute deviation fit to the orthogonal plane. These methods are outlined below.

It is natural to think of doing the standard least-squares fit of $\log r_e$ (hereafter LSQ; Guzmán et al. 1993; Bernardi et al. 2003), but early FP work mainly took $\log \sigma_0$ at the ordinate (Dressler et al. 1987; Djorgovski & Davis 1987; hereafter inverse LSQ) for their purposes. More recent work prefers the least-squares fitting of $\log r_e$ by minimizing the variance orthogonal to the FP plane (hereafter orthogonal least-squares fit, or OLSQ; Bernardi et al. 2003) or the least absolute deviations orthogonal to the plane (hereafter orthogonal least absolute deviation fit, or OLAD; Jørgensen et al. 1996; Pahre et al. 1998b). The orthogonal fitting has an advantage over other methods, reducing the systematic error by treating the variables symmetrically (Isobe et al. 1990). However, the orthogonal methods yield larger measurement errors than the LSQ methods, especially for small samples (Isobe et al. 1990).

Therefore, we also estimated the FP coefficients by taking the bisector, or the plane equidistant from the planes obtained through the standard LSQ and inverse LSQ (hereafter the LSQ bisector). We performed 1000 Monte Carlo samplings of subsets of early-type galaxies from Bernardi et al. (2003) to derive the FP coefficient errors on a sample of 50 early types to justify our approach. Through the sampling, we found the errors of the FP coefficients to be $(\sigma_a, \sigma_b) = (0.14, 0.06)$, best reproduced with the LSQ bisector method, while the other orthogonal methods gave overestimated errors ($\gtrsim$50% for the coefficient a). Aside from the error estimates, all three symmetrized methods reproduce the FP coefficient a of Bernardi et al. (2003) and the K-band early-type galaxy sample of Pahre et al. (1998b) within 5% agreement. On the other hand, the standard and inverse LSQ methods are found to have about minus and plus 20% systematic biases in the coefficient a estimates, respectively, in comparison to the symmetrized methods. Given these results, we adopted the FP coefficients with the LSQ bisector method as our base result.

TABLE 2
CONSTRUCTED FUNDAMENTAL PLANES AT VISIBLE THROUGH MIR

λ (1)	a (2)	b (3)	c (4)	r (5)
0.55	1.23 ± 0.10	−0.86 ± 0.04	−9.16 ± 0.40	0.96
2.2	1.42 ± 0.11	−0.81 ± 0.05	−8.20 ± 0.41	0.95
3.6	1.55 ± 0.11	−0.89 ± 0.04	−9.89 ± 0.39	0.96
4.5	1.47 ± 0.11	−0.92 ± 0.04	−10.16 ± 0.41	0.96
5.8	1.57 ± 0.13	−0.92 ± 0.05	−10.55 ± 0.50	0.95
8.0	1.55 ± 0.14	−0.75 ± 0.05	−9.30 ± 0.60	0.93

NOTES.—Fundamental planes for the sample of 56 galaxies with the $r_e > 2''$ cut using the LSQ bisector method. Col. (1): wavelength in μm. Cols. (2)–(4): Plane coefficients a, b, and c with associated uncertainties. Col. (5): Linear correlation coefficient.

4. RESULTS

In Table 2 we list the FP coefficients with errors from 1000 bootstrap resamplings (unless obtained directly from known error estimates, e.g., LSQ methods) derived from the LSQ bisector method, for wavelengths of 0.55–8.0 μm. We further plot the result of the FP fit in Figure 1, overlaid on the data points. We caution readers to focus less on the absolute values of (a, b) and more on the trend of the values with wavelengths or methods (see discussion at the end of this section and § 2). Gathering the outcomes, we are led to the wavelength-dependent nature of the FP coefficients, with (a, b) values getting close to the virial expectation of (2, -1) as the wavelength increases. Such a tendency has been noted before (Pahre et al. 1998a; Scodeggio et al. 1998), but our result indicates that it extends to 3.6 μm, and possibly beyond. When each cluster was analyzed separately, we also find the trend.

The wavelength dependence of the FP coefficients is further presented in Figure 2, where they are plotted using five different fitting methods (§ 3.2). The tilt of the FP is maximally reduced toward the virial expectation at IRAC bands, and the thickness of the FP is maintained thin for all but beyond 5.8 μm. In terms of the methodology, we confirm the analysis of § 3.2—the three symmetrized fittings give coefficient a values that are fairly consistent with each other (considering the sample size).

To quantify the wavelength dependence, we model the change of coefficient a as a linear function of wavelength by simultaneously fitting the OLSQ, OLAD, and the LSQ bisector results as follows:

$$da/d\lambda = 0.11 \pm 0.04\ \mu\mathrm{m}^{-1}, \quad (2)$$

from the visible to 3.6 μm (coefficient a behavior is flat afterward). This relation nicely explains the difference in coefficient a of 0.05 in the SDSS g^* to z^* bands (Bernardi et al. 2003). Meanwhile, for b, the tendency is not as linear as that for a, but has a local maximum near the K band, approaches closest to −1 at the IRAC 3.6–5.8 μm bands, and increases again at 8.0 μm. We attribute this behavior at 8.0 μm to the lower S/N, as well as the complexity in the 8.0 μm emission which can be dominated by the dust emission in some cases (Bressan et al. 2006; Ko & Im 2007). Indeed, the 8.0 μm FP has the largest scatter among IRAC bands. The above result, together with the tendency of coefficient b from Table 2, implies that the increases in coefficients a and b are $(\Delta a, \Delta b) \simeq (0.34, -0.03)$ from V band to 3.6 μm, and $(\Delta a, \Delta b) \simeq (0.15, -0.08)$ from K band to 3.6 μm. If we use the FP coefficients from the references in Figure 2 as the base values on which to apply equation (2), we obtain (a, b) ≃ (1.6–1.8, −0.9) at 3.6 μm, which is quite close to the virial expectation. The implication of this result is discussed in the next section.

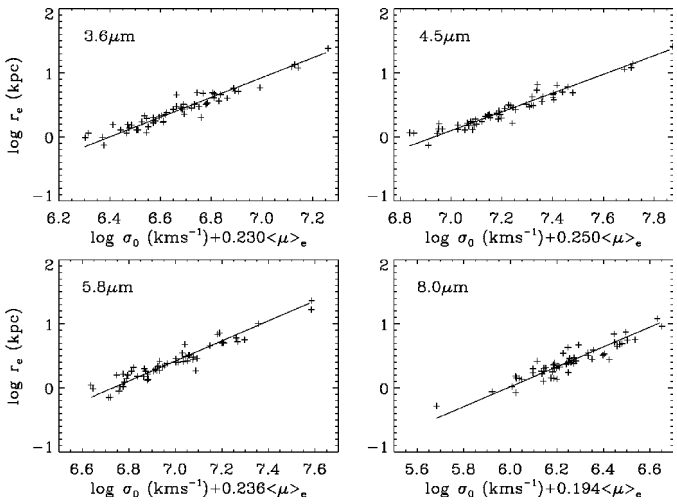

FIG. 1.—Constructed fundamental planes projected in the direction of smallest scatter at 3.6, 4.5, 5.8, and 8.0 μm, respectively.

Note that our coefficient a in K band, derived from a subsample of 56 early types from Pahre et al. (1998b), is smaller than the value derived from their full sample of 251 early types by $\Delta a = -0.11$. The discrepancy should be mostly due to the limited sample size. More than half of our MIR galaxies belong to the Coma Cluster (29 objects), and the Coma Cluster galaxies in Pahre et al. (1998b) show coefficient a in the K band ($a = 1.33$) smaller than the total sample result by $\Delta a = -0.20$, consistent with the results of Mobasher et al. (1999). Apart from the wavelength dependence, our results seem to be skewed toward the FP of the Coma Cluster.

5. IMPLICATIONS FOR THE ORIGIN OF THE FP TILT

Recent studies suggest that the FP tilt originates mostly from a systematic variation in the mass-to-light ratio (Cappellari et al. 2006; Bolton et al. 2007). However, the cause for the mass-to-light ratio variation is uncertain: it could be due to the stellar population, or the central dark matter fraction (Bolton et al. 2007). Also, some studies suggest that the tilt is mostly explained by the nonhomology related to the variation in the

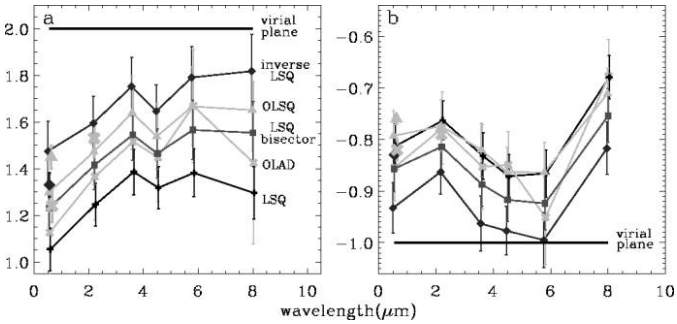

FIG. 2.—Wavelength dependence of coefficients a and b; diamond, triangle, square, cross, and plus sign symbols correspond to methodologies of inverse LSQ, OLSQ, LSQ bisector, OLAD, and ordinary LSQ, respectively. Connected lines with spacing for identification are from our catalog, while solitary symbols are from other literature (Dressler et al. 1987; Jørgensen et al. 1996; Pahre et al. 1998b; Bernardi et al. 2003) of nearby samples with $N \gtrsim 100$. Virial plane values assuming constant M/L are (a, b) = (2, −1). [*See the electronic edition of the Journal for a color version of this figure.*]

Sérsic index n among early-type galaxies (Trujillo et al. 2004). Here we discuss the implication of our result on these issues.

First, we investigated which one of the parameters—size or luminosity—dominates the observed change in the FP coefficients with increasing wavelength. This was done by deriving the FP coefficients from the MIR sample by replacing (1) r_e values or (2) $\langle I \rangle_e$ values with those from the shorter wavelength data (in our case the K band). The result is presented in Figure 3 (*left*), showing that the luminosity effect is the dominant factor up to 5.8 μm. Interpretation at 8.0 μm is difficult due to low S/N and dust emission. Our result suggests that the stellar population effect is significant going from K band to IRAC bands.

Next, we examined to what extent the stellar population plays a role in the FP tilt through the dynamical mass-to-light ratio $M_{\rm dyn}/L \propto r_e\sigma_0^2/L \propto \sigma_0^2/(r_e\langle I \rangle_e)$ (e.g., Bernardi et al. 2003) variation calculated from the FP coefficients. If $M_{\rm dyn}/L \propto L^{\beta}$, then $r_e \propto \sigma_0^{2/(1+2\beta)}\langle I \rangle_e^{-(1+\beta)/(1+2\beta)}$. The study of Trujillo et al. (2004) suggests $\beta \simeq 0.27$ based on the visible FP. Our result is that the FP coefficient reaches $a \simeq 1.6$–1.8 at 3.6 μm (§ 4). In such a case, this relation gives $\beta \simeq 0.06$–0.13, which enables us to explain more than half of the tilt in the visible FP. Moreover, the reduced tilt in the mass plane ($a_{\rm MP} - a_{\rm FP} = 0.27$: Bolton et al. 2007) is consistent with our $\Delta a = 0.30 \pm 0.11$ from the I band to the 3.6 μm in equation (2), advocating that the $M_{\rm dyn}/L$ variation is reduced by the regular light distributions in the MIR. As for the origin of the FP tilt, these results add another piece of evidence against the significance of nonhomology (Padmanabhan et al. 2004; Cappellari et al. 2006; Bolton et al. 2007), which predicts no change in the tilt with wavelength.

We also derived the β parameter by directly fitting the $M_{\rm dyn}/L$ ratio. Figure 3 (*right*) demonstrates that the observed dependence of $M_{\rm dyn}/L$ on L decreases and becomes flatter at IRAC bands, just like the changes in β derived from the FP coefficients. Combined with the fact that the change in the FP tilt with wavelength is dominated by the luminosity change, our $M_{\rm dyn}/L$-fit result suggests that the rest-frame MIR luminosities at 3.6–5.8 μm better represent the stellar mass than the shorter wavelengths, somewhat in agreement with Temi et al. (2008) but not so with Lacey et al. (2008). Among many possibilities, a proper combination of the metallicity and the age variation can possibly reproduce the observed trend, and we plan to investigate as future work the physical origin of the $M_{\rm dyn}/L$-L relation as a function of wavelength.

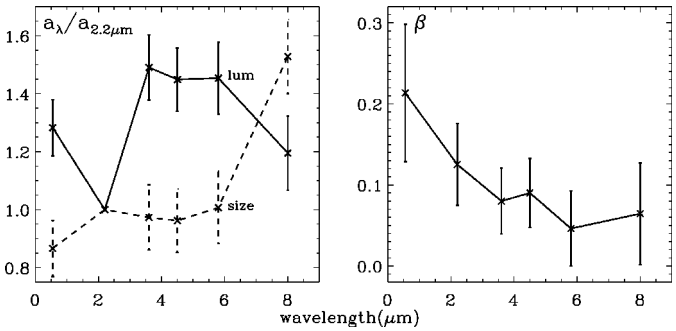

FIG. 3.—*Left*: Size vs. luminosity test on the FP coefficient a. The solid line (labeled "lum") is for the set of coefficients computed by exchanging the $\langle I \rangle_e$ data of each wavelength with that from the K band, while the dashed line (labeled "size") is the similar result computed by exchanging the r_e data. *Right*: Wavelength dependence of $M_{\rm dyn}/L$ on L as represented by the parameter β of $M_{\rm dyn}/L \propto L^{\beta}$ (see § 5).

6. SUMMARY

We studied the MIR fundamental plane relation of 56 early-type galaxies and derived the wavelength dependence of the FP coefficients. When the FP is expressed as $r_e \propto \sigma_0^a \langle I \rangle_e^b$, we found that the exponent on σ_0, a, increases as a function of wavelength as $da/d\lambda = 0.11 \pm 0.04$ μm^{-1}, while b reaches closest to -1 without systematic variation with wavelength. When the FP coefficients of previous studies are adopted as the starting point to calculate the MIR FP coefficients, we found that $(a, b) \simeq (1.6$–$1.8, -0.9)$ which is closer to the virial expectation, and that the change is dominated by the luminosity change. Together with the reduced dependence of the $M_{\rm dyn}/L$ ratio on L at MIR wavelengths, our outcomes suggest that the variation in the stellar population is responsible for a significant portion of the FP tilt, and that the rest-frame MIR better probes the stellar mass of low-redshift early-type galaxies than the shorter wavelengths.

This study was supported by a grant (R01-2007-000-20336-0) from the Basic Research Program of the Korea Science and Engineering Foundation, and by the Seoul Science Fellowship (H. J.). We thank the referee for useful comments, and Youngmin Seo and Soonyoung Min for algorithmic and technical advice in data analysis.

REFERENCES

Bernardi, M., et al. 2003, AJ, 125, 1866
Bertin, E., & Arnouts, S. 1996, A&AS, 117, 393
Bolton, A. S., Burles, S., Treu, T., Koopmans, L. V. E., & Moustakas, L. A. 2007, ApJ, 665, L105
Bressan, A., et al. 2006, ApJ, 639, L55
Bruzual, G., & Charlot, S. 2003, MNRAS, 344, 1000
Cappellari, M., et al. 2006, MNRAS, 366, 1126
Djorgovski, S., & Davis, M. 1987, ApJ, 313, 59
D'Onofrio, M., Valentinuzzi, T., Secco, L., Caimmi, R., & Bindoni, D. 2006, NewA Rev., 50, 447
Dressler, A., Lynden-Bell, D., Burstein, D., Davies, R. L., Faber, S. M., Terlevich, R. J., & Wegner, G. 1987, ApJ, 313, 42
Fazio, G. G., et al. 2004, ApJS, 154, 10
Fitzpatrick, E. L., & Massa, D. 2007, ApJ, 663, 320
Guzmán, R., Lucey, J. R., & Bower, R. G. 1993, MNRAS, 265, 731
Isobe, T., Feigelson, E. D., Akritas, M. G., & Babu, G. J. 1990, ApJ, 364, 104
Jørgensen, I., Franx, M., & Kjærgaard, P. 1996, MNRAS, 280, 167
Ko, J., & Im, M. 2007, AAS Meeting, 211, 96.03
Lacey, C. G., Baugh, C. M., Frenk, C. S., Silva, L., Granato, G. L., & Bressan, A. 2008, MNRAS, in press (astro-ph/0704.1562)
Laureijs, R. J., Helou, G., & Clark, F. O. 1994, in ASP Conf. Ser. 58, The First Symposium on the Infrared Cirrus and Diffuse Interstellar Clouds, ed. R. M. Cutri & W. B. Latter (San Francisco: ASP), 133
Mobasher, B., Guzman, R., Aragon-Salamanca, A., & Zepf, S. 1999, MNRAS, 304, 225
Padmanabhan, N., et al. 2004, NewA, 9, 329
Pahre, M. A. 1999, ApJS, 124, 127
Pahre, M. A., de Carvalho, R. R., & Djorgovski, S. G. 1998a, AJ, 116, 1606
Pahre, M. A., Djorgovski, S. G., & de Carvalho, R. R. 1998b, AJ, 116, 1591
Robertson, B., Cox, T. J., Hernquist, L., Franx, M., Hopkins, P. F., Martini, P., & Springel, V. 2006, ApJ, 641, 21
Scodeggio, M., Gavazzi, G., Belsole, E., Pierini, D., & Boselli, A. 1998, MNRAS, 301, 1001
Temi, P., Brighenti, F., & Mathews, W. G. 2008, ApJ, 672, 244
Treu, T., Koopmans, L. V. E., Bolton, A. S., Burles, S., & Moustakas, L. A. 2006, ApJ, 640, 662
Trujillo, I., Burkert, A., & Bell, E. F. 2004, ApJ, 600, L39